Wave Cancellation Experiments using a 1:10 Scale Cycloidal Wave Energy Converter

Casey Fagley[1], Stefan Siegel[1,#] and Jürgen Seidel[1]

1 Atargis Energy Corporation, 3185 Janitell Road Ste 101
Corresponding Author / E-mail: Stefan.Siegel@Atargis.com, TEL: +1-719-214-8815 x101

KEYWORDS : Wave Energy, Deep Water Wave, Wave Terminator, Wave Energy Converter, Cycloidal Wave Energy Converter

A 1:10 scale model of a Cycloidal Wave Energy Converter (CycWEC) was tested in the Texas A&M Offshore Technology Research center wave basin. These experiments were the first investigations involving a CycWEC in which three dimensional wave diffraction effects were present due to the fact that the span of the CycWEC was much smaller than the width of the basin. These experiments were also the first in which the power extracted from the waves exceeded the viscous losses leading to a measured net shaft power production of 370W. Direct shaft power measurements were found to agree well with expected CycWEC performance based on wave gauge measurements in connection with predictions of viscous losses based on published hydrofoil data. A three dimensional diffraction model predicted the observed surface wave patterns in the experiment well, and showed that diffraction induced wave focusing increased the recoverable wave power beyond the 2D predictions for small CycWEC spans. Overall the results from the 1:10 scale testing lead to higher performance estimates for a full scale CycWEC than what was predicted from earlier two dimensional simulations and smaller scale experiments.

NOMENCLATURE

S = span of the WEC blades,   Experiment: S=4.5m

C = Chord length of the WEC blades, Experiment: C=0.75m

H= Wave Height [m]

λ = Wave Length [m]

η=Water surface elevation

k= Wave Number

T = Wave Period

R = WEC Radius

y_c=Submergence depth of WEC shaft [m]

x,z = horizontal coordinates aligned with wave basin [m]

1. Introduction

Among alternative energy sources, wave power is one of the most abundant sources on earth. The World Energy Council according to Boyle [1] has estimated the world wide annual amount of wave power energy at 17.5 PWh (Peta Watt hours = 10^{12}kWh). This amount of power is actually comparable to the annual worldwide electric energy consumption, which is currently estimated at 16 PWh. Thus, wave power has the potential to provide a large portion of the world's electric energy needs, if it can be harnessed efficiently. In addition to the energy availability, wave power has other advantages. Since a large portion of the world's population lives close to the ocean shores, the distance between energy production and consumption is small, this reduces transmission losses and necessary investments in transmission lines. As opposed to other alternative energy sources like wind, stream and solar energy, the installation of wave power devices does not require use of already precious real estate. This makes wave power an ideal energy source for efficiently providing renewable energy to densely populated coastal areas. Ocean waves have a tremendous potential to provide clean renewable energy.

Further engineering aspects of wave power as an energy source are appealing as well. While the power density of both solar and wind in typical favorable sites is in the order of 1 kW/m^2 [2], wave power in a typical North Atlantic wave that was considered in a related paper [3] (wave height of H=3.5m and period of T=9s) yields 108 kW/m of wave crest. As shown there, a device extending about 40m in the vertical direction can extract almost all of this wave power, yielding a power density of about 2.7kW/m^2 or more than two and a half times that of wind or solar power. If one considers the theoretical inviscid conversion limits for waves and wind, which are 100% for waves [4] and 59% for wind [5], the accessible power density of waves is more than four times as large as that of wind. Furthermore, wave energy is available on a more consistent basis and can be better predicted in

advance, therefore mitigating the need to back up a wave power plant with other conventional power sources, such as is the case for solar and wind energy.

2. Background and Motivation

Analysis of the different wave energy conversion devices that have been investigated or proposed reveals a number of commonalities in design. The first is that all devices require a connection to the sea bed in order to extract energy, which has two main drawbacks. First, a seabed connection makes the device vulnerable in rough seas and storms, in the same way as an anchored ship is vulnerable in a storm (and will likely break the anchor line). According to Boyle [1], storm survivability has been a major problem for many wave energy converters, with some being destroyed by the elements as early as during deployment. Also, for most of the devices, the load imposed onto the seabed connection is proportional to the power which the device can extract. This means that the anchor point needs to be stronger and thus more costly as more energy is being extracted. Therefore, many of these devices cannot easily be scaled up to industrial power plant levels of energy conversion. In addition, since the devices need to be anchored to the sea floor, they are not well suited to operation in deep water waves, where the ocean floor may be hundreds of meters away from the surface. However, most wave energy is contained in deep water waves, and the energy density of a wave decreases as it approaches shallow water. Thus, most devices cannot operate in the most promising locations for wave power extraction.

Beyond survivability, efficiency has been a major issue for many WEC designs. While wave energy as a resource may be free, the construction effort to harness it is a major expense and to a large degree determines the cost of energy being produced. As a less efficient WEC will need to be larger in size to extract the same amount of energy as a more efficient one, cost of energy is directly related to efficiency. Arguably, the most efficient WEC is one that can extract all of the energy from an incoming wave, and the class of wave energy converters that is able to achieve this is commonly referred to in literature as wave termination devices. There have been various wave termination designs reported in literature, with the most well-known devices being the Salter Duck [6] and the Bristol or Evans Cylinder [7]. Both consist of a series of elements which are aligned parallel to the wave crests, in the case of the Salter Duck these are cam-shaped and floating on the surface, while the Bristol Cylinder is fully submerged. Both have been shown to be able to absorb an incoming wave completely. The wave energy is converted to electric power by means of a power-take-off system that is hydraulic in both cases. As both devices move at approximately the wave induced water velocity, the devices need to feature a large surface area to convert appreciable amounts of power. This increases construction cost, reduces storm survival odds and has ultimately motivated the investigation of the CycWEC described here. The fact that both devices require mooring to the ocean floor also hampers storm survival odds and precludes installation in very deep water.

A typical Cycloidal wave energy converter as considered in this paper is shown in Figure 1. It features one or more hydrofoils attached eccentrically to a main shaft at a radius R. While the shaft rotates, the pitch angle of the blades may be adjusted. This device operates at a rotational speed of the hydrofoil that is typically an order of

magnitude larger than the wave induced water velocity, and employs the lift force at the hydrofoil to generate shaft torque directly. Using lift allows for a much smaller hydrofoil plan form area to be employed compared to the cross sectional areas of Duck and Cylinder, and generating shaft torque directly eliminates the need for a costly and inefficient hydraulic power take off system. In addition, it is conceptually possible to join several CycWECs into a cluster where the reactive forces at the shaft can be made to cancel, which reduces or negates entirely the need for mooring and thus enables deep water deployment while improving storm survival odds (see [8] for sketches). The fact that the reactive force changes direction though 360 degrees with each wave passage enables force cancellation if the individual WECs are spaced half a wavelength apart, thus causing reactive forces of same magnitude but opposite direction.

A single rotating hydrofoil was first investigated by Hermans et al. [9] both numerically and experimentally. While Hermans et al. reported very low wave energy conversion efficiencies (on the order of a few percent), Siegel et al. [3] were able to show in simulations that with improved sizing of the WEC as well as by using synchronization of the rotation of the foil with the incoming wave, wave termination with better than 99% inviscid efficiency was possible. These numerical findings were confirmed by 1:300 scale experiments in 2011, as reported by Siegel et al. [10] where inviscid conversion efficiencies of greater than 95% were achieved in a small, 1:300 scale two dimensional wave flume. Both of these initial studies performed synchronization of the WEC with a numerically generated harmonic wave, or a paddle wave maker, respectively. Thus they did not require a feedback controller and estimator to succeed. A controller and estimator were for the first time successfully implemented by Jeans et al. [11] for irregular waves in a numerical simulation. Typical conversion efficiencies in this study were beyond 90% for a superposition of two harmonic waves, and around 80% for irregular waves following a Bretschneider distribution. At the same time, the controller and estimator were successfully tested in an experiment as reported in [12] where harmonic waves with different wave heights and frequencies were successfully cancelled, achieving efficiencies comparable to the earlier synchronization experiments that had a priori knowledge of the incoming wave. The performance of the feedback controller and estimator could thus be experimentally verified for the first time.
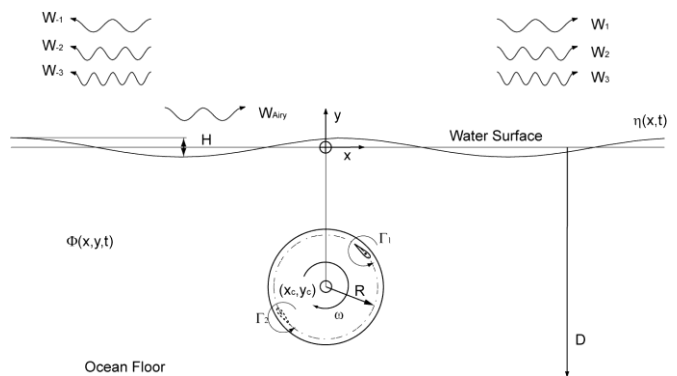
Figure 1: CycWEC Sketch

In this paper an experimental investigation was performed at a scale of 1:10 in the Texas A&M Offshore Technology Research Center

wave basin. The dimensions of the model were a 1 meter radius and a 4.5 meter blade span. The WEC was attached to a split main shaft driving two 3.5 kW generators. Feedback control was utilized to synchronize the rotation of the WEC to the incoming waves as well as to adjust the pitch of the blades to the incoming wave height. This paper presents results achieving for the first time net shaft power production. The experiments presented here were also the first investigations in a 3D wave basin, where the span of the blades was much shorter than the width of the basin. To estimate the impact of finite span on the performance of the WEC, a simple numerical wave propagation model was developed to estimate the wave pattern. Validation of the numerical model using wave gauge measurements is presented, both for wave generation and wave energy conversion experiments. Subsequently, the numerical model is used to estimate the impact of different finite spans and wave height ratios on the CycWEC performance.

2.1 3D Wave Model

The surface elevation η_c of a circular wave can be described as:

$$\eta_c(x, z, t) = H(r) \sin(\omega t - kr)$$

With x and z the horizontal coordinates, k the wave number, r the distance from the wave center, ω the wave period and t time. If this wave is to conserve energy as it radiates outward, the wave height H has to decrease with distance from the wave generator. A height function that does conserve wave energy resulting in a reduced wave height as the wave propagates away from the wave center is given as,

$$H(r) = \sqrt{\frac{H_0^2 \, r_0}{4r}}$$

where the initial wave height is specified as H_0 at a finite distance r_0 from the center. It is possible to use several, point source circular waves to approximate the wave pattern caused by more finite span wave generators. For a CycWEC, the waves generated can be approximated as a sum of individual circular wave generators arranged along a line of finite length equal to the span S of the WEC blades.

$$\eta_{WEC}(x, z, t) = \sum_{n=1}^{N} \eta_{cn} \, , x > 0$$

$$\eta_{WEC}(x, z, t) = 0 \, , x < 0$$

Single sided wave generation is assumed and assured by setting the WEC wave to zero for negative x coordinates. This has been proven numerically, experimentally at 1:300 scale, and is experimentally verified at 1:10 scale in following sections. The N circular wave generators are located between z=-S/2 and z=S/2 along x=0. A number of N=25 individual circular waves was found to produce converged results. The strength of each circular wave generator used to discretize the WEC wave generation was approximated by an elliptical distribution.

$$H_0(z) = H_c \sqrt{1 - \left(\frac{z}{2S}\right)^2}$$

This modeled the lift distribution along the span of the foil which caused a wave height that was proportional to the local circulation. To assure that the maximum wave height at the center of the foil was H_c, the overall generated wave height was renormalized to the value specified. The wave field generated by the WEC was then superimposed with the wave field generated by the incoming wave. The incoming wave in this investigation was a long crested Airy wave traveling in the positive x direction modeled as

$$\eta_A(x, z, t) = H \sin(\omega t - kx)$$

The final surface elevation was then calculated by superimposing the incoming airy wave with the wave generated by the WEC

$$\eta_A(x, z, t) = \eta_A + \eta_{WEC}$$

2.2 Control Volume analysis

The wave field resulting from the interaction of incoming Airy wave and the waves generated by the circular waves used to model the WEC were used to determine the overall energy absorbed by the WEC. Using a control volume that enclosed the WEC completely, the fundamental waves entering and leaving that control volume could be calculated. To ease calculations, the control volume chosen was a rectangle aligned with the coordinate sytem axes. The circular waves were decomposed in a x and z component. Thus, the portion of each circular wave leaving the control volume boundaries could be calculated at each location along the boundaries. For an Airy wave, wave power P per unit length can be calculated as

$$P = \frac{\rho g}{8} H^2 C_g$$

Where Cg is the wave Celerity, ρ the density of water and g the gravity constant. Thus the wave power traversing a control volume boundary extending in the z direction from z_1 to z_2 could be calculated.

$$P = \int_{z_1}^{z_2} \sum_{m=1}^{M} P_{mx}(z) dz$$

$$P_x(z) = \frac{\rho g}{8} (H_x{}^2 + H_z{}^2) C_{gx}$$

The subscripts indicate the vector component of the respective quantity in that direction. These equations can be modified to calculate the power traversing across a horizontal control volume boundary by swapping the subscripts x and z. The overall amount of power extracted by the WEC could then be calculated by choosing a closed rectangular control volume.

To determine the efficiency with which the WEC extracted energy from the waves, a reference quantity equal to the wave power of the Airy wave times the span of the WEC was used. Thus, if the control volume analysis showed that this amount of energy was extracted from the waves, the efficiency was unity or 100%. Any efficiency larger than this indicated that diffraction induced wave focusing was

encountered.

3. Experimental Setup

3.1 Wave Basin

All experiments reported here were conducted at the Texas A&M University Offshore Technology Research Center (OTRC) wave basin. The basin was 45.7m in length, 30.5m in width and had a water depth of 5.8m. A set of 48 hinged flap wave makers, individually controlled by hydraulic cylinders, spanned one of the short sides of the basin. At the other end, a progressive wave absorber consisting of stacked screens acted as an artificial beach to reduce reflection of incoming waves. The wave maker had a maximum design wave height of H_{WM}=0.9m at a wave period of T=2.5s. This wave was a deep water wave with a wave length of λ=10m and thus determined the model scale of 1:10 compared to a full scale deep ocean design wave for the CycWEC. While current and wind generators were available, they were not used in the present investigation
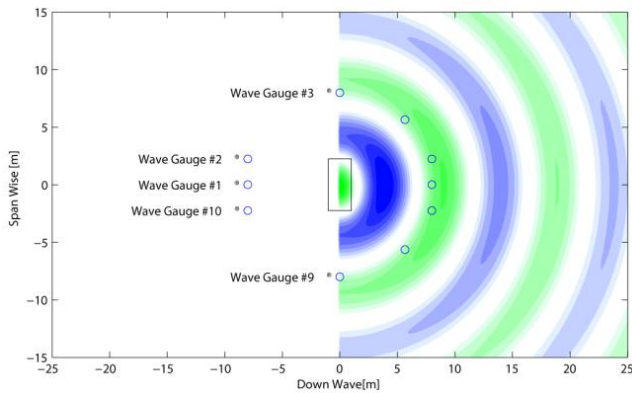
Figure 2: Instantaneous surface elevation for a wave generation simulation. WEC model is shown to scale as a rectangle, and the wave gauge locations which are consecutively numbered in clockwise direction are shown.

In order to investigate the surface wave pattern caused by the WEC and its interaction with incoming waves, a set of 10 wire type capacitive wave gauges were installed at a distance of 8m from the shaft of the WEC. The locations of the wave gauges are shown in Figure 2. The wave gauge calibration was estimated to be accurate to within 1mm of water level. For all waves generated, a calibration was performed with the model removed from the water in order to assure that the wave heights at the model location matched the target values. For this calibration, a wave gauge was placed at the center of the model.

3.2 Cycloidal WEC Model

The CycWEC model, shown in a CAD rendering in Figure 3, was designed specifically to efficiently interact with the wave climate in the OTRC tunnel. It featured two hydrofoils with a chord length C=0.75m and span S=4.5m. The hydrofoils had a NACA0015 cross section with a curved camberline that matched the radius R=1m at which they were attached to the main shaft. End discs with a height of 10cm were installed at the ends to minimize tip vortex losses. The hydrofoils were attached to a split main shaft by means of two struts

located at the ends of the hydrofoils. The struts were equipped with linear actuators allowing for control of the hydrofoil pitch. Each of the struts was streamlined using a NACA 0015 section.

Figure 3: CAD model of CycWEC 1:10 scale model on floor mount

The main shafts were connected to two individual motor/generator units installed in a water proof enclosure. These consisted of a 3 Phase 230V AC 3.7kW asynchronous motor coupled to an 80:1 gear box. The shafts were instrumented to allow for direct measurement of the shaft torque by means of two load cells. The load cells were calibrated by the manufacturer and delivered an accuracy of 0.05% of their full scale reading, which coincided with the maximum motor torque. The motors were operated by four quadrant capable inverters allowing for software control of torque, speed and position. Breaking resistors allowed for dissipation of the regenerative power produced during wave power extraction. As the inverters were operated over a CANOpen network, pertinent parameters such as shaft position, velocity and motor current were reported back to the control computer and logged in sync with all other data. The motor current readings had a resolution of 0.1% of the nominal motor current. While the motors themselves were installed in water proof enclosures, the respective inverters were located in an electronics rack located on the bridge spanning the tunnel. This rack also accommodated the control computer used for feedback control of the WEC as well as for data acquisition and logging. Both the motor shafts, as well as the WEC shaft were instrumented with incremental rotary encoders for position feedback. These inverters were also linked to allow for synchronous rotation of both shafts.

A mounting frame allowed for attachment of the WEC to hard points in the tunnel floor. While this provided a fixed horizontal positioning of the WEC in the tunnel, the WEC model itself could be traversed in the vertical direction by means of two lead screws operated by gear motors, which allowed for access to the model when lifted above the water line and adjustment of the submergence depth of the model during operation. The range of motion was -1.8m<y_c<1.2m and could be controlled with an accuracy of a fraction of a millimeter. Figure 4

shows the CycWEC model installed on the frame in the OTRC tunnel, while lifted out of the water.

Figure 4: CycWEC 1:10 scale model installed in OTRC wave tunnel. The WEC is lifted above the water line during installation in this picture.

All communication with motor controllers, pitch actuators and data acquisition was accomplished through a CAN bus network under a CANOpen software protocol. The feedback control software was run on a PC and written in LabVIEW, operating at an update rate of 20ms. All data logged during the experimental runs was synchronized using the CANOpen SYNC message ensuring that the measurements were taken at the same instants of time. The SYNC message also provided hardware based timing for the control loop providing feedback to the CycWEC.

4. Results

Based on the recognition that efficient wave termination requires generation of a wave of equal amplitude and period, but exactly out of phase with the incoming wave, the first experiments conducted were concerned with wave generation and are reported in the next section. After wave generation was established, one of the wave gauges located up-wave of the WEC was used as input to a feedback controller to operate the CycWEC exactly out of phase with the incoming wave to achieve wave cancellation. The results from these experiments are reported in the following section.

4.1 Wave generation

All earlier experiments with this type of Cycloidal Wave Energy Converter were conducted in a 2D wave flume, where the blades of the WEC spanned the entire width of the flume. The waves generated in these experiments were straight crested and of equal wave height along the span of the blades. They also maintained their wave height traveling the length of the flume. Initial observations of the surface wave pattern in the OTRC facility showed a drastically different wave pattern, an example of which is shown in Figure 5. The WEC in this picture is rotating in the counter clockwise direction, and an almost circular wave pattern on the left side of the WEC can be observed. While not easily visible in the picture, the waves also show a decreasing height as they radiate away from the WEC. On the right side of the WEC, little to no waves were observed matching the observations from the 2D wave flume experiments.
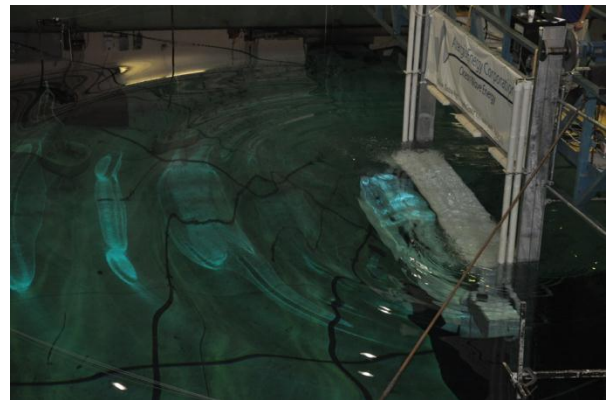
Figure 5: Picture of surface elevation for a wave generation experimental run.
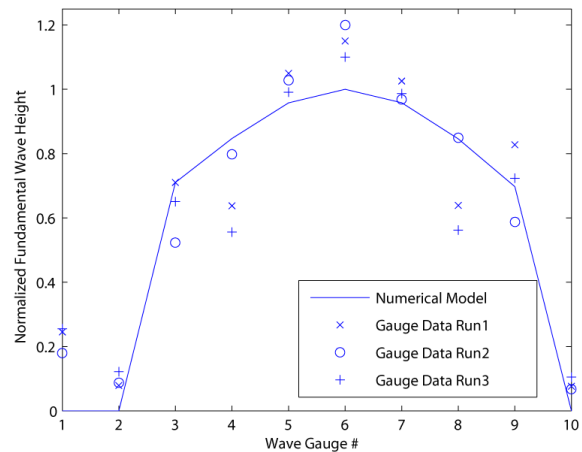
Figure 6: Comparison of wave gauge measurements to numerical diffraction model wave heights. Wave period T=2.5s

To gather a fundamental understanding of the impact of this three dimensional wave pattern on the performance of the CycWEC, a simple wave radiation model as described in section 2.1 was developed. An instantaneous snapshot of the wave pattern generated using this model is shown in Figure 2. While the horizontal direction is reversed in the model snapshot compared to the experimental picture, a good qualitative match between both can be observed. In order to provide a more quantitative comparison, the wave heights

measured by the wave gauges were compared to the wave heights from the numerical model as shown in Figure 6. It can be observed that the numerical model provided accurate predictions of the wave heights generated. Differences between model and wave gauge measurements were most likely attributable to wave reflections encountered in the experiments. These reflections were caused both by reflections from the basin side walls causing transverse waves, as well as longitudinal waves due to less than perfect absorption of the longitudinal waves at the screens acting as wave absorbers. Furthermore, the paddle wave makers would re-reflect any incoming waves since they had no active wave absorbing capabilities.

As outlined in earlier publications (e.g. [3]), the ability to create a single sided wave is an important prerequisite to enable wave termination. This capability of the CycWEC was maintained in the present experiments at 1:10 scale, and agreed well with earlier experiments and simulations. Figure 6 provides experimental evidence to that effect, as can be seen by comparing the wave heights at wave gauges located up-wave of the CycWEC (#1, #2, and #10) to the wave heights on the opposite side of the CycWEC (#5, #6 and #7). The small wave heights measured up-wave of the WEC only manifest themselves once reflected waves reached the gauges, and were not present in the beginning of an experimental run right after the CycWEC was started. The impact of the almost circular wave pattern on CycWEC performance observed in the present experiments is discussed in detail in section 4.3.

4.2 Wave cancellation

The main focus of the present test campaign was to establish the ability of the CycWEC to extract power from incoming waves. In order to do so, the waves generated by the CycWEC (see previous section) need to be exactly 180 degrees out of phase with the incoming wave. To achieve this, a feedback controller utilized the signal from a wave gauge located up-wave in between wave gauges #6 and #7 (see Figure 2) to synchronize the rotation of the CycWEC with the incoming wave. The phase between this wave gauge signal and the rotation of the CycWEC was adjustable in software. There are various delays in this system, some of which could be determined a priori like the wave propagation delay from the wave gauge location to the CycWEC, while others had to be experimentally determined like the delay added due to the inverters achieving the demanded position with a time delay. To correctly account for all delays, a phase angle study was conducted the results of which are shown in Figure 7. It can be seen that the wave height at the two up-wave installed wave gauges #2 and #10 were almost constant and independent from the feedback phase, while the wave heights at the down-wave wave gauges showed a distinct minimum at a feedback phase of 245 degrees. This indicated that the CycWEC was operated exactly out of phase at this feedback phase angle. The reduction in wave height indicated that wave energy was extracted from the incoming wave.

While previous experiments and potential flow simulations were not able to measure the amount of power delivered to the CycWEC shaft directly, the present experiment had two independent means to determine shaft power. A load cell at each shaft measured shaft torque directly and ahead of gear box and motor/generator, while the motor inverter delivered a reading of motor current which was also indicative of shaft power. The sign convention for both quantities was chosen such that a positive sign indicated power delivered to the shaft from the motor, while a negative sign indicated that power was delivered from the shaft to the generator indicating power extraction

from the wave induced flow field. The two quantities were not identical due to power losses in the three stage gear box, as well as the efficiency of the generator itself. Furthermore, the relationship between current and shaft torque was not straightforward and linear for the 3 Phase asynchronous motor used, and also depended on the rotational speed of the motor.
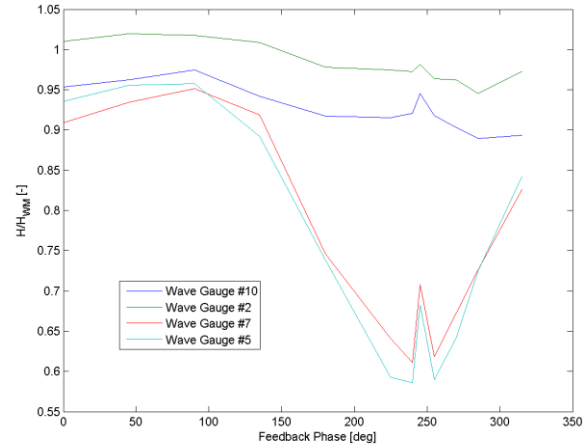
Figure 7: Wave heights as a function of feedback phase for the four wave gauges located up- and down wave of the WEC. $H_{WM} = 0.2m$, T=2.5s

The shaft power measurements corresponding to the phase angle study presented in Figure 7 are shown in Figure 8 as solid lines. Both the motor current and shaft torque showed a minimum for the same phase angle that was observed in the wave gauge measurements. While only one data set is shown here for brevity, the correlation between wave measurements and shaft power was found in all experiments conducted and validated our earlier approach to determine wave termination efficiency by means of wave height measurements.
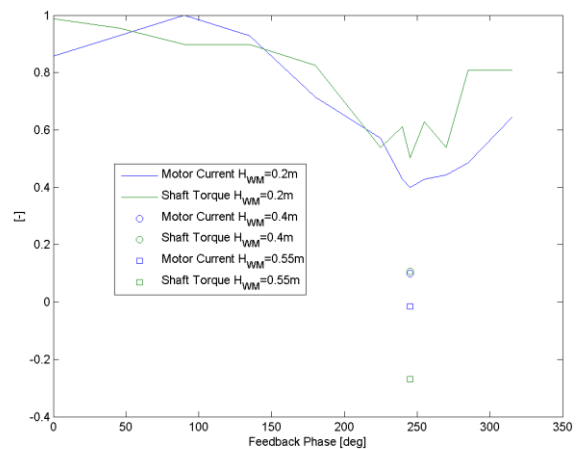
Figure 8: Non dimensional Shaft Power and Motor Controller Current as a function of feedback phase.

While the shaft torque and motor current were reduced at the wave height of 0.2m for which the phase study was conducted, no net shaft power was obtained. This was consistent with estimates of the power loss due to drag of the hydrofoils, which at the wave height of 0.2m was larger than the power extracted from the waves. Consequently, only a reduction of about 40% of the motor current was achieved at the optimal feedback phase of 245 degrees. With the optimal feedback phase established, the wave height produced by the basin wave maker was increased.

Figure 8 shows two additional wave heights, and it can be seen that at a wave height of 0.4m the net shaft power approached zero, while at a wave height of 0.55m which was chosen as the design point of the CycWEC in this experiment net shaft power was obtained. Both the wave height at which zero net power was obtained and the amount of power delivered to the shaft, which was 370W for 0.55m wave height; agreed with the estimates based on published hydrofoil lift and drag values and the associated viscous power loss.

A comparison of the measured wave heights from the wave gauges, as well as the predictions from the numerical diffraction model are shown in *Figure 9*. With the exception of wave gauge #6 the agreement is found to be very good, the discrepancy is most likely due to reflected waves from the basin side walls as discussed above.
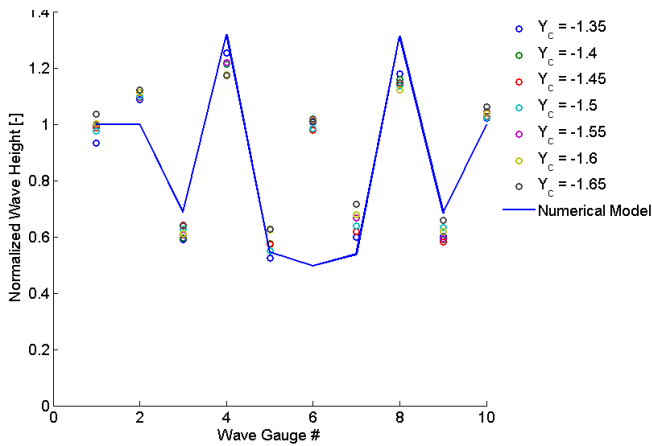
Figure 9: Wave Heights during wave cancellation with power production as a function of wave gauge location in comparison to numerical model. Shown are experimental runs for various submergence depths y_c.

4.3 Further 3D diffraction model results

With the validity of the 3D diffraction model introduced in section 2.1 experimentally verified, it was possible to analyze the effect of diffraction on the CycWEC performance, as well as to investigate the impact of parameters that could not easily be changed in the experiment on the performance. In this section additional results from the numerical diffraction model are presented, and analyzed using a control volume approach to determine the amount of power extracted from the waves by the CycWEC. In addition, the ratio between the span of the CycWEC and the incoming wave length was varied. This would require a change of the length of the CycWEC blades in the experiment, which is very difficult to perform with a model of this size but could be achieved easily using the numerical diffraction model.
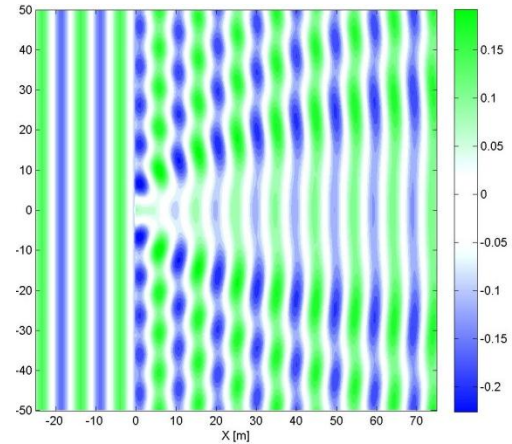
Figure 10: Instantaneous surface elevation for a wave cancellation simulation at the model span ratio of S/λ = 0.45 and an incoming wave height of H=0.3m and T=2.5s

Figure 10 shows a snapshot of instantaneous water surface elevation during a wave cancellation simulation run. The incoming wave traveled left to right, and the CycWEC was centered at (0,0) with the span of the blades aligned in the wave crest direction. Since the span of the WEC was significantly smaller than the wave length of λ=10m, strong diffraction effects can be observed causing the wake (region of reduced wave height) down-wave (or to the right in the figure) of the CycWEC to spread out at an angle of about 30 degrees in the z direction. This spreading was due to the almost circular wave generated by the CycWEC (shown in Figure 2) interacting with the straight crested incoming wave seen in the left portion of Figure 10. Diffraction also caused a modulation of the height of the wave crests outside of the wake region, leading to larger wave amplitudes than that of the incoming wave in particular right at the edge of the wake region (e.g. troughs at x=20 z=+-15m). Using control volume analysis, it was possible to determine the power extracted by the CycWEC by accounting for the power of all waves crossing the boundaries of the control volume. While the results were verified to be control volume size independent, a control volume extending from x=-20m to x=40m in the wave travel direction, and z=-40m to z=40m in the wave crest direction was used for this analysis. The power extracted by the CycWEC was then divided by the power of the incoming wave approaching the CycWEC times the span of the CycWEC. This efficiency we refer to as the 3D diffraction efficiency since it was only present if diffraction effects caused a spreading of the wake as seen in Figure 10. It could not be observed in 2D simulations or wave flume experiments of the type conducted earlier where the WEC blades spanned the width of the wave flume.

Figure 11 shows the 3D diffraction efficiency as a function of the non-dimensional span of the CycWEC. The efficiency increased as the non-dimensional span decreased, and remained above 100% for all span ratios investigated. At the non-dimensional span ratio of S/λ=0.45 of the present experiment, 3D diffraction effects increased the amount of wave power by about 40% beyond what could be achieved in a 2D wave flume or simulation. The 3D diffraction efficiency of the CycWEC approached 100% from above for large span to wavelength ratios, and thus approaches the 2D limit.
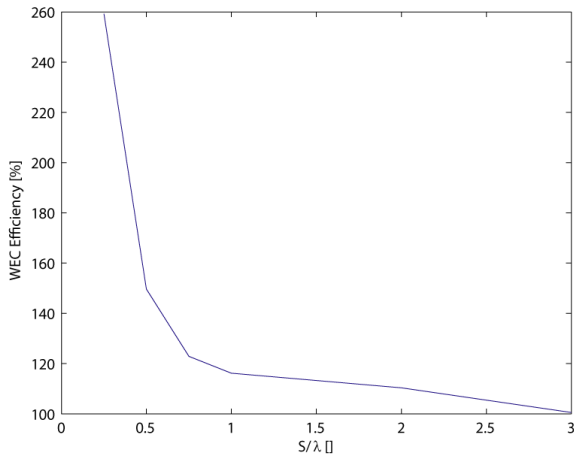
Figure 11: WEC 3D Diffraction efficiency as a function of span to wavelength ratio. The optimal WEC center wave height is used for each span ratio.

For very small span to wavelength ratios, there was a dramatic wave focusing induced increase in efficiency achieved, for the smallest S/λ ratio of 0.25 the WEC efficiency reached values beyond 250%. While this was consistent with wave focusing effects observed for point absorbers, it would not be easily achievable with the CycWEC device investigated here since the hydrofoil aspect ratio would become very small, at which point the lift generation of the hydrofoil would be greatly reduced due to induced tip losses. This effect was not modeled in the wave propagation simulation results shown.
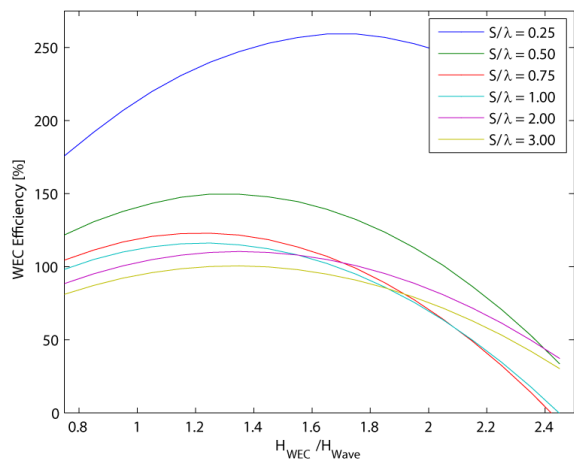
Figure 12: WEC Efficiency as a function of WEC center wave height to incoming wave height ratio

One additional parameter that could be adjusted in the diffraction model was the wave height of the wave generated by the CycWEC. Since an elliptical lift and thus wave generation distribution along the span of the hydrofoil was assumed, the average lift along the span was $\pi/4$ times the lift at the center of the hydrofoil. Conversely, the center wave height needed to be $4/\pi$ or about 1.27 times the average desired wave height or lift. Figure 12 shows that for larger span to

wave length ratios, the optimal efficiency was achieved at this value, indicating that the average wave height produced by the WEC needed to match the wave height of the incoming wave. For very small span to wave length ratios, though, a much larger wave height produced by the CycWEC was needed to achieve optimal efficiency. This result made intuitively sense since the diffraction effects spread the wave height produced by the WEC in the span wise direction to a much larger span than that of the WEC.
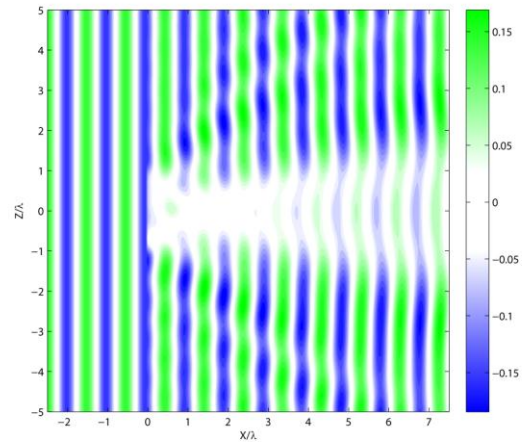
Figure 13: Instantaneous surface elevation for a wave cancellation simulation at the model $S/\lambda = 2.00$

The impact of WEC span on the angle at which the diffracted waves were spreading could be observed by comparing a small WEC span as shown in Figure 10 to a large span shown in Figure 13. The angle at which the wake was spreading was greatly reduced in Figure 13, demonstrating how the large span WEC approached the results seen in 2D simulations and wave flume experiments by reducing diffraction effects.

CONCLUSIONS

We present experimental results from 3D wave tank experiments of a Cycloidal Wave Energy Converter at a scale of 1:10. The model featured two hydrofoils of 0.75m chord and 4.5m span attached at a radius of 1m to a central shaft. The power at the shaft of the CycWEC was measured directly by two independent means with good agreement. The water surface elevation around the CycWEC was measured using capacitive wire wave gauges. The CycWEC was operated both without incoming waves observing the wave pattern generated, as well as with incoming waves where power was extracted from the waves. Due to the small span to wave length ratio, strong 3D diffraction effects were observed in both experiments. For the first time, net shaft power production of 370W at the design point of the CycWEC was achieved. A good correlation between shaft power and wave height reduction was found, validating earlier wave cancellation experiments and simulations employing control volume analysis.

In order to understand and isolate the impact of diffraction on the CycWEC performance, a simple 3D diffraction model was developed based on linear circular point wave source superposition. The model agreed well with measured wave heights in the experiment, and

showed that wave diffraction induced wave focusing increased the wave power that could be extracted beyond the two dimensional limit. This indicated that while the CycWEC avoided the losses due to up-wave radiated waves suffered by typical symmetric point absorbers, it could nonetheless leverage the benefits of diffraction induced wave focusing at small span to wave length ratios.

ACKNOWLEDGEMENTS

DISCLAIMER

This report was prepared as an account of work sponsored by an agency of the United States Government. Neither the United States Government nor any agency thereof, nor any of their employees, makes any warranty, express or implied, or assumes any legal liability or responsibility for the accuracy, completeness, or usefulness of any information, apparatus, product, or process disclosed, or represents that its use would not infringe privately owned rights. Reference herein to any specific commercial product, process, or service by trade name, trademark, manufacturer, or otherwise does not necessarily constitute or imply its endorsement, recommendation, or favoring by the United States Government or any agency thereof. The views and opinions of authors expressed herein do not necessarily state or reflect those of the United States Government or any agency thereof.

REFERENCES

[1] Boyle, G., 2004. Renewable Energy - Power for a sustainable future. Oxford University Press.

[2] Bedart, R., 2005. Final summary report - offshore wave power feasibility demonstration project. Tech. rep., E2I EPRI Global, WP 009 - US Rev 1.

[3] Siegel, S. G., Jeans, T., and McLaughlin, T., April 2011. "Deep ocean wave energy conversion using a cycloidal turbine". Applied Ocean Research, Volume 33 Issue 2, pp. 110–119.

[4] Evans, D. V., 1976. "A theory for wave-power absorption by oscillating bodies". J. Fluid Mech., 77(1), pp. 1–25.

[5] Betz, A., 1920. "Das Maximum der Theoretisch moeglichen Ausnuetzung des Windes durch Windmotoren". Zeitschrift fuer das gesamte Turbinenwesen, 26, p. 307309.

[6] Salter, S. H., 1989. "World progress in wave energy - 1988". International journal of ambient energy, 10(1), pp. 3–24.

[7] Evans, D. V., Jeffrey, D. C., Salter, S. H., and Taylor, J. R. M., 1979. "Submerged cylinder wave energy device: theory and experiment". Applied Ocean Research, 1(1), pp. 3–12.

[8] Siegel, S. G., filed in 2006, awarded 2010. "Cyclical wave energy converter". U. S. Patent 7,686,583 and pending / awarded International Patent applications.

[9] Hermans, A. J., van Sabben, E., and Pinkster, J., 1990. "A device to extract energy from water waves". Applied Ocean Research Computational Mechanics Publications, Vol. 12, No. 4, p. 5.

[10] Siegel, S. G.; Fagley, C. & Nowlin, S. "Experimental wave termination in a 2D wave tunnel using a cycloidal wave energy converter". Applied Ocean Research Vol. 38, pg. 92-99, 2012

[11] Jeans, T., Siegel, S. G., Fagley, C., and Seidel, J., 2011. "Irregular deep ocean wave energy conversion using a cycloidal wave energy converter". In 9th European Wave and Tidal Energy Conference (EWTEC), Southampton, UK, September 5th -9th, 2011.

[12] Siegel, S., Fagley, C., Roemer, M., and McLaughlin, T., 2011. "Experimental wave cancellation using a cycloidal wave energy converter". In 9th European Wave and Tidal Energy Conference (EWTEC), Southampton, UK, September 5th -9th, 2011.